Neuropsychopharmacology (2014) 39, 3067–3076

www.neuropsychopharmacology.org

Dopamine Modulation of GABAergic Function Enables Network Stability and Input Selectivity for Sustaining Working Memory in a Computational Model of the Prefrontal Cortex

Sergio E Lew[1] and Kuei Y Tseng*[,2]

[1]Instituto de Ingeniería Biomédica, Facultad de Ingeniería, Universidad de Buenos Aires, Buenos Aires, Argentina; [2]Department of Cellular and Molecular Pharmacology, The Chicago Medical School at Rosalind Franklin University of Medicine and Science, North Chicago, IL, USA

Dopamine modulation of GABAergic transmission in the prefrontal cortex (PFC) is thought to be critical for sustaining cognitive processes such as working memory and decision-making. Here, we developed a neurocomputational model of the PFC that includes physiological features of the facilitatory action of dopamine on fast-spiking interneurons to assess how a GABAergic dysregulation impacts on the prefrontal network stability and working memory. We found that a particular non-linear relationship between dopamine transmission and GABA function is required to enable input selectivity in the PFC for the formation and retention of working memory. Either degradation of the dopamine signal or the GABAergic function is sufficient to elicit hyperexcitability in pyramidal neurons and working memory impairments. The simulations also revealed an inverted U-shape relationship between working memory and dopamine, a function that is maintained even at high levels of GABA degradation. In fact, the working memory deficits resulting from reduced GABAergic transmission can be rescued by increasing dopamine tone and vice versa. We also examined the role of this dopamine–GABA interaction for the termination of working memory and found that the extent of GABAergic excitation needed to reset the PFC network begins to occur when the activity of fast-spiking interneurons surpasses 40 Hz. Together, these results indicate that the capability of the PFC to sustain working memory and network stability depends on a robust interplay of compensatory mechanisms between dopamine tone and the activity of local GABAergic interneurons.
Neuropsychopharmacology (2014) **39,** 3067–3076; doi:10.1038/npp.2014.160; published online 23 July 2014

INTRODUCTION

Dopamine innervation in the prefrontal cortex (PFC) originates from the ventral tegmental area (Lindvall *et al*, 1974; Sesack *et al*, 1998; Thierry *et al*, 1978), a pathway that is critical for the regulation of cognitive functions including working memory and decision-making (for review, see Floresco, 2013). The neurobiology underlying the modulation of these PFC functions is thought to be mediated by dopamine's ability to enable context relevant inputs to enhance the activity of selective neuronal ensembles for hundreds of milliseconds to seconds (Funahashi *et al*, 1989; Goldman-Rakic, 1995). In addition to the role of D1 and NMDA receptors in facilitating prefrontal output responses (Baldwin *et al*, 2002; Flores-Barrera *et al*, 2013; Floresco and Phillips, 2001; Gurden *et al*, 1999; Jay, 2003; Tseng and O'Donnell, 2005), dopamine action in the PFC includes activation of fast-spiking interneurons (FSIs) (Gorelova *et al*, 2002; Tseng and O'Donnell, 2007b). They are a subset of GABAergic interneurons critical for determining the timing and spatial selectivity of pyramidal cell firing (Rao *et al*, 2000). Accordingly, it has been suggested that FSI could shape the response pattern of prefrontal pyramidal neurons to mesocortical dopamine drive (Tseng *et al*, 2006; Tseng and O'Donnell, 2004). For example, ventral tegmental area stimulation frequently results in suppression of pyramidal cell activity in the PFC, an inhibitory response that matches the temporal course of local prefrontal FSI excitation (Lewis and O'Donnell, 2000; Tseng *et al*, 2006). At the cellular level, there is ample evidence that part of the inhibitory action of dopamine in the PFC is due to an enhancement of local GABAergic tone (Gorelova *et al*, 2002; Gulledge and Jaffe, 1998; Pirot *et al*, 1992; Tseng *et al*, 2006; Tseng and O'Donnell, 2004). In fact, GABAergic interneurons in the PFC do express dopamine receptors (Le Moine and Gaspar, 1998; Mrzljak *et al*, 1996; Muly *et al*, 1998; Vincent *et al*, 1995) and FSI excitability becomes positively modulated by D1 and D2 receptors in the adult PFC, a functional maturation that occurs late in adolescence (Tseng and O'Donnell, 2007b). Thus, a fine tuning between local PFC GABAergic transmission and pyramidal cell firing

*Correspondence: Dr KY Tseng Department of Cellular and Molecular Pharmacology, The Chicago Medical School at RFUMS, office #2.172, 3333 Green Bay Road, North Chicago, IL 60064, USA, Tel: +1 847 578 8655, Fax: +1 847 578 3268,
E-mail: kuei-yuan.tseng@rosalindfranklin.edu
Received 26 November 2013; revised 3 June 2014; accepted 26 June 2014; accepted article preview online 30 June 2014

by dopamine has been proposed to have a critical role in the regulation of working memory processes as disruptions of such interactions are implicated in the pathophysiology of cognitive deficits observed in schizophrenia and related psychiatric conditions (Lewis and Gonzalez-Burgos, 2006; O'Donnell, 2011; Tseng *et al*, 2009). Furthermore, deficits in PFC GABAergic function can result in reduced cognitive flexibility as shown in animal models (see review by Floresco, 2013). We therefore hypothesize that dopamine-dependent facilitation of FSI function in the PFC is needed to improve the signal detection ratio between task-dependent stimuli and distractors by enhancing clusters of neuronal activity that encode such stimuli. Here, we employed a modified version of the well-established computational model of working memory developed by Brunel and Wang (2001) to determine how dopamine modulation of FSI transmission in the PFC enables input selectivity in pyramidal cells to sustain working memory and its reset. The latter will be simulated by a transient phasic elevation of dopamine that is sufficient to cause rapid increases in FSI activity.

MATERIALS AND METHODS

Our computational model is a modified version of that introduced by Brunel and Wang (2001) with the inclusion of a dopamine component on GABAergic interneurons (see equation (10)). Briefly, a PFC network (Figure 1) of 2000 cells composed by 80% pyramidal neurons and 20% FSI was modeled. Two subsets of 240 pyramidal neurons respond selectively to input stimuli S1 or S2 (S-responding neurons). The remaining 1120 pyramidal neurons belong to a cluster of non-selective (NS) responding cells. Per simulation, 100 independent trials were run for each condition using parameters that were adjusted to avoid potential ceiling/floor effects, especially to modifications of dopamine and GABA. Changes in neuronal firing rate were estimated using a non-overlapping window of 25 ms. Differential equations were determined by an integration time step of $dt = 0.01$ ms.

The membrane potential V_m results from the integration of external and recurrent excitatory and inhibitory currents:

$$C_m \frac{dV_m(t)}{dt} = -g_m(V_m(t) - V_L) - I_{syn}(t) \quad (1)$$

$C_m = 0.5$ nF/0.2 nF is the membrane capacitance whereas $g_m = 25$ nF/20 nF and $V_L = -70$ mV account for the leakage conductance and leakage potential for excitatory/inhibitory neurons, respectively. If V_m surpasses the threshold potential $V_{TH} = -50$ mV, an action potential is elicited, and the membrane potential is held at the reset potential $V_r = -55$ mV for the duration of the refractory period (2.5 ms for pyramidal neurons and 1.5 ms for FSI).

Synaptic currents for both pyramidal neurons ($I_{syn\text{-}pyr}$) and FSI ($I_{syn\text{-}FS}$) were computed as follows:

$$I_{syn-pyr}(t) = I_{AMPAext}(t) + I_{AMPArec}(t) + I_{NMDArec}(t) + I_{GABA}(t) + I_{D1-NMDA}(t)$$

$$I_{syn-FSI}(t) = I_{AMPAext}(t) + I_{AMPArec}(t) + I_{NMDArec}(t) + I_{GABA}(t) + I_{D1-NMDA}(t) + I_{DA}(t)$$

$AMPA_{ext}$, $AMPA_{rec}$, and $NMDA_{rec}$ account for AMPA and NMDA receptor-mediated currents resulting from external and recurrent glutamatergic drive. The inhibitory tone from FSI originates from GABA-A receptor-mediated transmission. Dopamine modulation of neuronal activity in the developmentally mature PFC network is modeled by including both the well-documented D1-positive modulation of NMDA receptor-mediated response ($I_{D1\text{-}NMDA}$) and the facilitatory action of D1 and D2 receptors on FSI excitability (I_{DA}) (Tseng and O'Donnell, 2004, 2005, 2007b).

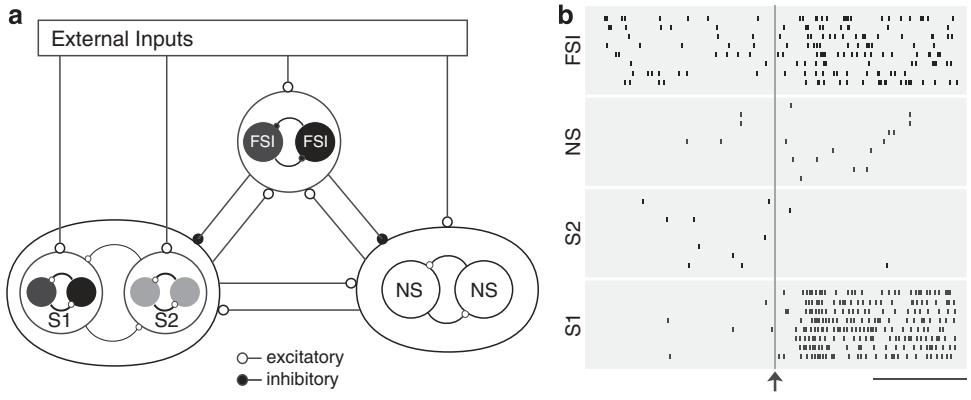

Figure 1 (a) The PFC model is comprised by groups of selective (S) and non-selective (NS) pyramidal neurons, and fast-spiking inhibitory interneurons (FSIs). The group of S-responding pyramidal neurons is composed by two clusters of 240 cells each that respond selectively to input stimuli S1 and S2, respectively. Synaptic connections among pyramidal neurons within each of the S-responding group are stronger ($w = 1.9$) than those between S1- and S2-responding cells ($w = 0.84$). A synaptic efficacy of $w = 1$ was used for connections within NS pyramidal neurons and FSI, and between pyramidal neurons (both S and NS) and FSI. The global inhibitory tone is provided by FSI with a synaptic efficacy of $w = 1$. (b) Raster of cell firing showing examples of neuronal activity across the different populations before and after input stimulus S1 (indicated by the arrow and gray line; calibration bar: 250 ms).

AMPA and GABA-A currents are computed as follows:

$$I_{AMPAext}(t) = g_{AMPAext}(V(t) - V_E)\sum_{j=1}^{Cext} s_j^{AMPAext}(t)$$

$$I_{AMPArec}(t) = g_{AMPArec}(V(t) - V_E)\sum_{j=1}^{C_E} w_j s_j^{AMPArec}(t)$$

$$I_{GABA}(t) = g_{GABA}(V(t) - V_I)\sum_{j=1}^{C_I} w_j s_j^{GABA}(t)$$

where $g_{AMPAext} = 2.08$ nS/1.62 nS, $g_{\mathrm{AMPArec}} = 0.104$ nS/0.135 nS, and $g_{\mathrm{GABA}} = 1.25$ nS/0.973 nS are the nominal values for AMPA and GABA conductances for both excitatory and inhibitory neurons, respectively. $V_{\mathrm{E}} = 0$ mV and $V_{\mathrm{I}} = -70$ mV are the reversal potentials for excitatory and inhibitory cells, respectively. $S^{AMPAext}$, $S^{AMPArec}$, and S^{GABA} are action potential-driven variables that modulate the magnitude of the net conductances. The instantaneous values for recurrent conductances are also affected by the connectivity parameter, which is $w_j = 1$ between FSI and the three groups of pyramidal cells (S1, S2, and NS), and among pyramidal neurons of the NS group. The connectivity parameter is $w_j = 1.9$ among neurons within the same S-responding group and $w_j = 0.84$ between the two S-responding groups (see Figure 1).

The nominal value of the NMDA current is modulated by a voltage-dependent Mg^{2+} block of the channel.

$$I_{NMDArec}(t) = (1 + \phi_{D1-NMDA}) \times \frac{g_{NMDA}(V(t) - V_E)}{1 + [Mg^{2+}]\exp(-0.062V(t))/3.57} \times \sum_{j=1}^{C_E} w_j s_j^{NMDA}(t) \quad (5)$$

where $g_{NMDA} = 0.327$ nS/0.258 nS is the NMDA conductance for excitatory/inhibitory neurons, respectively and $\phi_{D1\text{-}NMDA}$ accounts for the D1 facilitation of NMDA currents (see equation (9)).

Action potential-driven variable s accounts for the dynamics of AMPA and NMDA conductances. Fast conductances for AMPA- and GABA-mediated transmission were modeled as exponential functions:

$$\frac{ds_j^{AMPA}(t)}{dt} = -\frac{s_j^{AMPA}(t)}{\tau_{AMPA}} + \sum_k \delta(t - t_j^k) \quad (6)$$

$$\frac{ds_j^{GABA}(t)}{dt} = -\frac{s_j^{GABA}(t)}{\tau_{GABA}} + \sum_k \delta(t - t_j^k) \quad (7)$$

For NMDA conductances, we used the following differential equation:

$$\frac{ds_j^{NMDA}(t)}{dt} = -\frac{s_j^{NMDA}(t)}{\tau_{NMDAdecay}} + \alpha x_j(t)(1 - s_j^{NMDA}(t))$$

$$\frac{dx_j(t)}{dt} = -\frac{x_j(t)}{\tau_{NMDArise}} + \sum_k \delta(t - t_j^k)$$

Here, Kronecker's delta (δ) is the epoch for the onset of presynaptic spikes whereas τ is the time constant, $\tau_{AMPA} = 2$ ms, $\tau_{GABA} = 5$ ms, $\tau_{NMDArise} = 2$ ms, and $\tau_{NMDAdecay} = 100$ ms. In the model, the number of spikes arriving from external inputs follows a Poisson function with a basal λ value of 2400 spikes/s. Thus, λ value increases only in selective neurons in response to stimulus presentation, a function that is determined by the stimuli contrast, which is typically 10% in our simulations (Supplementary Figure 1). In this regard, when a stimulus with a given contrast value c is presented, an increase in λ (defined as $c.\lambda$) will be applied only to those inputs that were previously defined as selective for the S-responding cells.

To simulate the D1 action on pyramidal neurons and FSI cells, the $\Phi_{D1\text{-}NMDA}$ was included in equation (9), a variable that depends on basal dopamine levels (Brunel and Wang, 2001).

$$\Phi_{D1-NMDA}(t) = 0.1\tanh(DA - \varphi) \quad (9)$$

where DA is the dopamine level and φ is a parameter that shifts the sigmoid function depending on the cell type ($\varphi = 1$ for pyramidal cells and $\varphi = 1.05$ for FSI) as in Brunel and Wang (2001).

The dopamine modulation of FSI activity was computed by means of a Na^+ conductance-like current with a reversal potential of $V_{DA} = 55$ mV:

$$I_{DA}(t) = g_{DA}(V_m(t) - V_{DA}) \quad (10)$$

Here, changes in dopamine levels were simulated by modifying the basal $g_{DA} = 0.35$ nS conductance in a linear-dependent manner. This basal g_{DA} value was chosen to maintain FSI activity in the adult PFC within physiological ranges as seen *in vivo* (Tseng *et al*, 2006).

To test how the model responds to selective stimuli, we simulated the presentation of one of the selective stimuli S for 250 ms followed by a delay of 1 s, and computed the following measures:

$$\text{Stimulus selectivity}: \quad d' = \frac{|\mu_{FRS1} - \mu_{FRS2}|}{\sqrt{\frac{\sigma_{FRS1}^2 + \sigma_{FRS2}^2}{2}}} \quad (11)$$

$$\text{Working memory index}: WMI = \frac{\mu_{FRS1} - \mu_{FRS2}}{\mu_{FRS1} + \mu_{FRS2}} \quad (12)$$

Both the mean firing rate (μ_{FRSi}) of S-responding neurons and its variance ($\sigma^2{}_{FRSi}$) were taking into account. For d', μ_{FRSi} and $\sigma^2{}_{FRSi}$ were calculated from the stimulus presentation period whereas the *WMI* was obtained from a 250-ms window at the end of each trial 500 ms after the stimulus offset.

RESULTS

Our PFC model comprises a network of 2000 neurons with an inhibitory/excitatory ratio of 0.25 (Figure 1), and includes the following physiological features of dopamine action: (i) dopamine facilitation of prefrontal GABAergic transmission *via* activation of local FSIs (Tseng and O'Donnell, 2007b); (ii) D1 facilitation of NMDAR-mediated response in both pyramidal neurons and FSI. We first determined the differential effects of transient steps of

dopamine elevation on the spontaneous activity of pyramidal neurons and FSI. For each simulation, changes in neuronal mean firing rate were estimated using a 25-ms non-overlapping window. Under basal dopamine tone, pyramidal neuron discharge activity was $\sim$0.8 Hz whereas the mean firing rate for FSI was $\sim$9 Hz. Consistent with the biological effects found in the PFC in response to phasic ventral tegmental stimulation *in vivo* (Tseng *et al*, 2006), the simulations revealed that increasing steps of dopamine (mimicking phasic dopamine) also elicited facilitation of FSI activity concurrent with a coordinated suppression of pyramidal cell firing (Figure 2a). In our model, a complete cessation of pyramidal cell activity was observed when a step of threefold dopamine increase and subsequent elevation of FSI activity by $\sim$35% were simulated. These results pointed toward a non-linear relationship between pyramidal cell activity and FSI function. Accordingly, a steady downregulation of local GABAergic tone (GABA degradation) exponentially increased the mean firing rate of pyramidal neurons (Figure 2b). Interestingly, the hyperactive state resulting from the reduced GABAergic inhibition can be normalized by augmenting basal dopamine levels (Figure 2c). Together, these results indicate that one critical mechanism to control pyramidal cell activity is the increased responsiveness of FSI to dopamine.

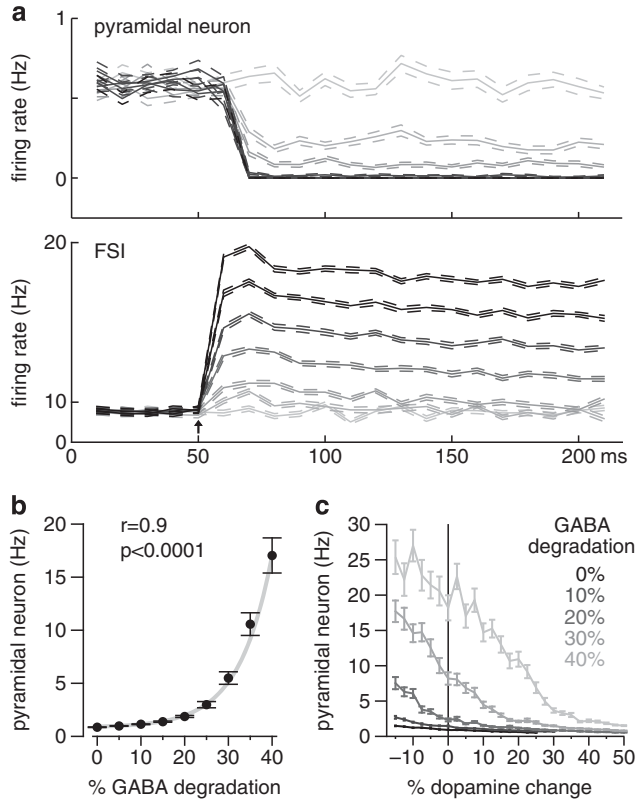

Figure 2 (a) FSI and pyramidal cells in the PFC exhibit opposite firing responses to increasing steps of dopamine level (from 0, 0.5, 1, 2, 3, 4, and 5 folds) above baseline. Black arrow indicates the onset of dopamine increase. (b) Impact of downregulation of local prefrontal GABAergic inhibitory tone (GABA degradation) on pyramidal cell activity. Note the exponential increase in pyramidal cell firing following GABA degradation >20%. (c) Relationship between basal dopamine tone and pyramidal cell firing at different degrees of GABA degradation.

We next assessed how changes in basal dopamine levels (from -10 to $+10$%) affect the ability of the PFC network to discriminate between stimuli by measuring *d'* (see Materials and Methods for details). In our model, there are two populations of pyramidal neurons that respond exclusively to external input stimuli S1 or S2 (Figure 3a). We first determined how different contrast values between S1 and S2 inputs (ranging from 5 to 80%) affect the *d'* discrimination curve (Supplementary Figure 1). Data from these simulations show that a minimal 10% contrast value is required to enable the emergence of a dopaminergic modulation of *d'*. Thus, input selectivity (computed as *d'*) is maximal under the basal dopamine state (Figure 3b) because S1-responding neurons typically increase their activity to S1, but remain unresponsive to S2 and vice versa (Figure 3c). Interestingly, such selectivity begins to diminish as dopamine tone moves away from baseline irrespectively of the direction of change (Figure 3b). Further analyses revealed that the deterioration of selectivity in the low dopamine state arises from an increased responsiveness of S1- and S2-responding pyramidal neurons to the non-preferred input stimuli (Figure 3c). This latter effect is likely due to an insufficient level of GABAergic inhibition needed to maintain network stability (Figure 2b and c) as similar degrees of diminished selective response can be obtained following GABA degradation (Figure 3d). Conversely, the reduced selectivity observed upon increasing levels of dopamine is due to an augmented GABAergic tone exerting a strong inhibition on both S1- and S2-responding pyramidal neurons to the preferred input stimuli (Figure 3c). In fact, GABA degradation effectively improves selectivity only in the high dopamine state as indicated by a right-shift of the normalized *d'* curve (Figure 3d). Together, these results indicate that a fine homeostatic interplay between dopamine function and local GABAergic transmission is required for maintaining PFC network stability and output selectivity.

Among the different PFC-dependent functions, working memory is of interest because it is associated with the ability of neuronal populations to sustain activity from hundreds of milliseconds to seconds in response to a cue presentation for solving a task several hundred of milliseconds later (Goldman-Rakic, 1995). Typically, such sustained activity is resistant to interferences produced by distractors, that is, task-independent stimuli capable of perturbing the correct response (Brunel and Wang, 2001). Thus, retention of cue-associated information over distractors is critical to correctly execute the task. Here, we simulated this paradigm and asked how working memory becomes affected by changes in dopamine and GABA functions. In each trial, 250 ms duration of S stimulus presentation is followed by a 300-ms delay interval before a distractor is turned on. For S1-responding pyramidal neurons the distractor was the S2 stimulus, and vice versa for S2-responding cells. Working memory retention was considered successful if the average activity of S-responding pyramidal neurons (measured 250 ms after the offset of the distractor) remained higher than the rest of the pyramidal cells. We first examined how changes in the functional connectivity among pyramidal neurons of the same S-responding group alter working memory. By increasing and decreasing the strengths of such connectivity, we found

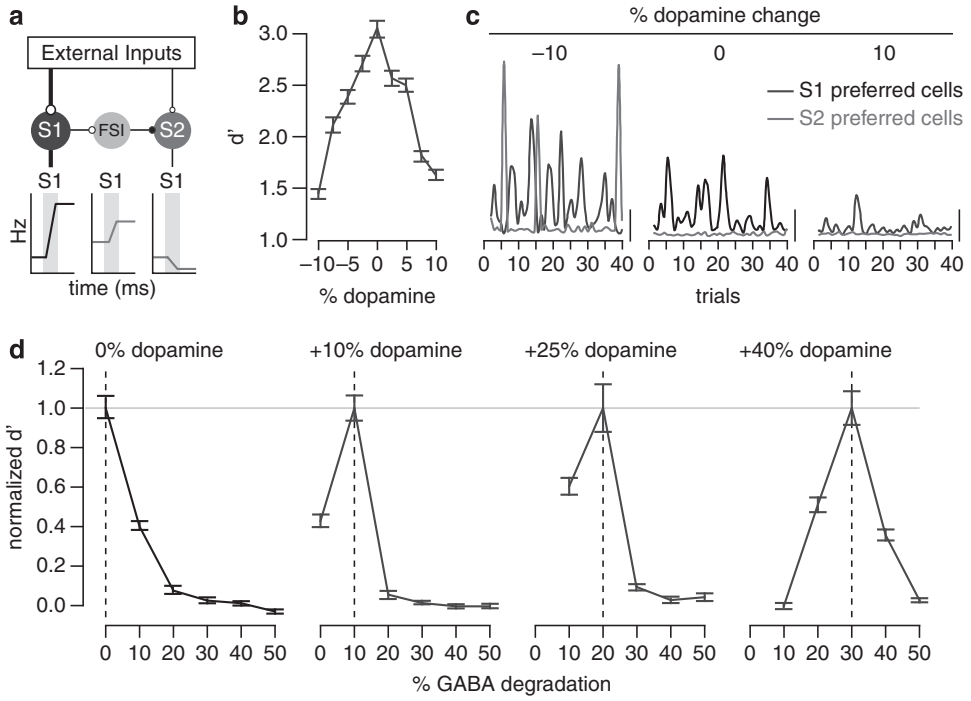

Figure 3 (a) Diagram of the PFC network highlighting the two populations of S-responding pyramidal neurons and their exclusive responsiveness to external input stimuli S1 or S2. In this example, activation of S1-responding pyramidal neurons results in inhibition of the S2-responding group through a fast-spiking interneuron (FSI) mechanism. (b) Relationship between basal dopamine tone and prefrontal discrimination of selective stimuli. The selectivity of the PFC response was determined by *d'*. Higher *d'* values reflect better selectivity as seen at baseline dopamine while decreasing or increasing dopamine tone deteriorate stimuli selectivity. (c) Examples of S1- and S2-responding pyramidal neurons activity during the presentation of S1 input stimulus at three levels of basal dopamine. Data show the mean firing rate of S1- and S2-responding cells across 40 trials (vertical calibration bars: 4 Hz). (d) Impact of GABA degradation on stimuli selectivity at increasing levels of basal dopamine (from 0 to +40% above baseline). Vertical dashlines indicate the % of GABA degradation associated with the highest degree of selectivity for each dopamine state. A full color version of this figure is available at the *Neuropsychopharmacology* journal online.

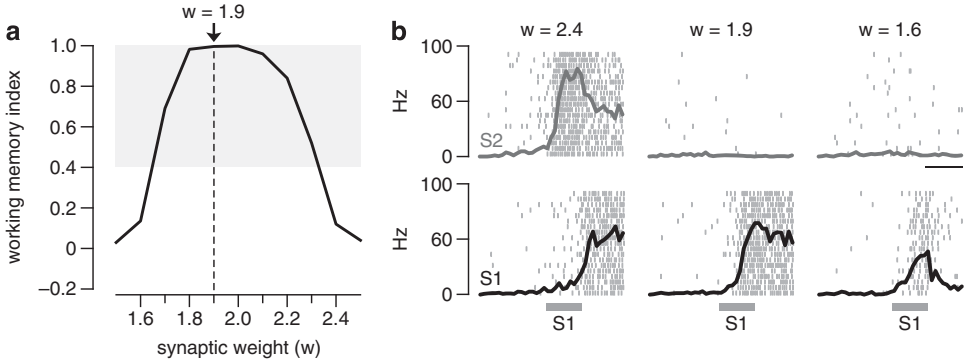

Figure 4 (a) Relationship between working memory performance (measured as working memory index, WMI) and changes in synaptic weight (*w*) among pyramidal neurons of the same S-responding group at baseline dopamine and GABA levels. Arrow indicates the original synaptic weight ($w = 1.9$) used in the simulations shown in Figures 2–4. Note that a reduction in the WMI occurs at both high and low values of *w*. (b) Examples of S1 (black)- and S2 (red)-responding pyramidal neurons' activity during and after the presentation of S1 stimulus (250 ms duration) showing the different mechanisms by which a change in *w* can diminish the WMI (horizontal calibration bar: 250 ms). Increasing values of *w* (eg, $w = 2.4$) eliminate the selectively of S-responding neurons whereas decreasing values of *w* (eg, $w = 1.6$) reduce the level of recurrent activity needed to maintain persistent neuronal firing. A full color version of this figure is available at the *Neuropsychopharmacology* journal online.

that the relationship between working memory and synaptic weights follows an inverted U-shape function (Figure 4a). Thus, only a range of synaptic weights favors retention of working memory by enabling sufficient input selectivity and recurrent excitation to sustain persistent activity in S-responding pyramidal neurons. This balance between input selectivity and recurrent activity becomes disrupted when too much or too little synaptic strengths were simulated, all of which prevent the formation of working memory (Figure 4b). Next, we investigated how changes in dopamine and GABA impact the retention of working memory (Figure 5). These simulations were conducted using a value of synaptic connectivity among S-responding pyramidal neurons that was sufficient to elicit working

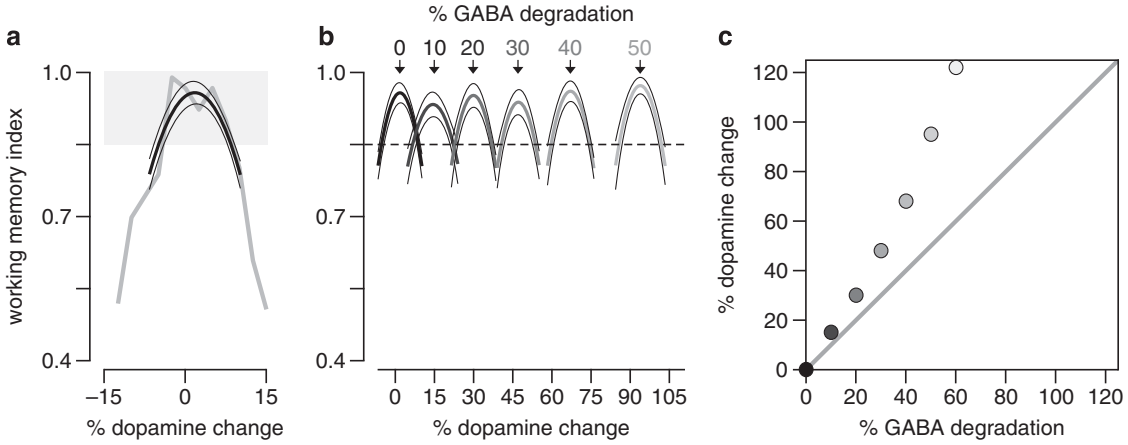

Figure 5 (a) U-shape relationship between basal dopamine tone and PFC working memory capacity (computed as working memory index) measured at normal GABA function. The synaptic weight among S-responding pyramidal neurons was 1.9 (see Figure 4). (b) In the presence of increasing levels of GABA degradation, a higher basal dopamine tone is needed to achieve working memory. Interestingly, the inverted U relationship between dopamine and working memory is maintained despite the GABA degradation. Thus, a particular combination of dopamine and GABA function is required to achieve optimal working memory performance (above the dashed line; working memory index >0.85). (c) Scatter plot summarizing the non-linear relationship between the degrees of GABA degradation needed to restore working memory equilibrium (arrows in b) in response to increasing levels of basal dopamine.

memory at baseline ($w=1.9$, Figure 4a). The data show that high values of working memory performance (ie, working memory index >0.85) can be achieved only within a particular combination of dopamine/GABA function (Figure 5a). Interestingly, we found an inverted U-shape relationship between working memory and dopamine tone, a function that is maintained while increasing the levels of GABA degradation (Figure 5b). In fact, the working memory deficits induced by GABA degradation can be rescued by increasing dopamine tone, resulting in a shift of the working memory index curve to the right (Figure 5b). Further analyses revealed a non-linear interplay between dopamine and GABA function in sustaining working memory stability in the PFC (Figure 5c).

We next determined whether phasic activation of FSI is sufficient to bring S-responding pyramidal cell firing back to baseline and reset PFC working memory. To test this, a step of transient dopamine increase (500 ms duration) above the baseline level was introduced after the selective stimulus S and once the S-responding pyramidal neurons had reached to a steady state of increased activity (Figure 6a). Results from the simulations show that phasic augmentation of dopamine (ie, fold change above baseline) can effectively decrease the elevated firing state of S-responding neurons in a concentration-dependent manner (Figure 6b). In fact, the ability of dopamine transients to reset the activity of S-responding cells is determined by the magnitude of inhibition elicited during the 500-ms phasic dopamine increase (Figure 6b). In our model, this inhibitory action is dictated by FSI (Figure 6c), whose level of responsiveness increases linearly to dopamine differentials (Figure 6d), and by the duration of the dopamine transient (Supplementary Figure 2). Interestingly, the extent of dopamine-induced FSI excitation needed to reset the S-responding neurons follows a non-linear function (Figure 6d). Further analyses revealed that the point of inflexion for the reset occurs when the activity of FSI surpasses 40 Hz (Figure 6e). Together, these results underscore the critical role of dopamine–FSI interaction in the regulation of working memory reset in the PFC.

DISCUSSION

Our PFC model predicts that behavioral outcomes associated with an initial dopamine elevation will increase FSI activity. As a result, the signal detection ratio in the PFC network increases by virtue of reduced recurrent activity in pyramidal neurons. Further simulations revealed that a fine homeostatic interplay between dopamine and FSI is needed to enable PFC output selectivity and stability. A similar dopamine–FSI interaction is required for the formation and retention of working memory, especially in the presence of distractor stimuli. Finally, our model also predicts that phasic activation of FSI by dopamine is an effective mechanism to reset the PFC working memory state back to baseline. Together, these results show for the first time that a critical gain of prefrontal FSI function by dopamine is necessary for maintaining PFC network stability, which enables working memory retention and reset.

A major inhibitory action of dopamine in the PFC results from local activation of GABAergic interneurons (Gorelova *et al*, 2002; Gulledge and Jaffe, 1998; Tseng and O'Donnell, 2004, 2007a, b). In the adult PFC, pharmacological stimulation of both D1 and D2 receptors converge to enhance FSI excitability (Tseng *et al*, 2008; Tseng and O'Donnell, 2007b). Hence, the net effect of mesocortical dopamine is to drive FSI and subsequently inhibit pyramidal output neurons. We simulated these interactions and found that the activity of pyramidal neurons in the PFC becomes inhibited following phasic dopamine increase. This is consistent with *in vivo* studies showing suppression of pyramidal cell firing following stimulation of the mesocortical dopamine pathway (Ferron *et al*, 1984; Jay *et al*, 1995; Lewis and O'Donnell, 2000; Pirot *et al*, 1992; Tseng *et al*, 2006). Although several mechanisms have been proposed to explain this inhibition,

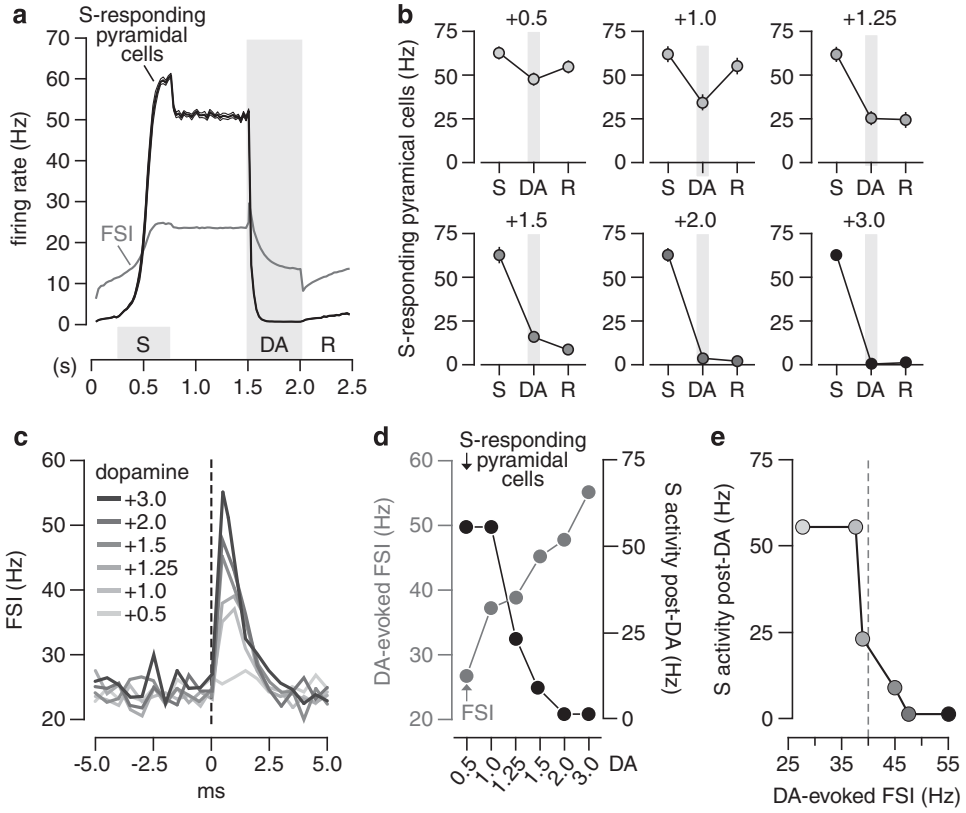

Figure 6 (a) Firing rate time course of S-responding pyramidal neurons and FSI during and after the selective stimulus S followed by a 500-ms step of dopamine (DA) increase. Here, a step of dopamine increase (3-fold above the basal tone) was used to inhibit and reset (R) the activity of S-responding pyramidal cells back to baseline values. (b) Summary of the effects of increasing dopamine levels from 0.5- to 3-fold above baseline on S-responding neuronal activity measured at 500 ms after the offset of the selective stimulus (S), 250 ms after the onset of the dopamine transient (DA), and 250 ms after the offset of the dopamine step (R). Note that while the degree of inhibition in S-responding cells is positively correlated with the dopamine transients, a critical level of inhibition is required to enable reset (ie, + 1.5 DA). (c) FSI response to increasing steps of dopamine transients (same as in b). Note the rapid, but transient increase in firing rate after the onset of the dopamine pulse (dashed line). (d) Relationship between dopamine transients and the FSI peak response or the mean firing rate of S-responding pyramidal neurons at 250 ms post-dopamine offset (ie, R from a). (e) Summary of the FSI peak response to dopamine steps and the mean firing rate of S-responding pyramidal neurons at 250 ms post-dopamine offset. A full color version of this figure is available at the *Neuropsychopharmacology* journal online.

paired recordings of interneurons and pyramidal cells revealed that a coordinated activation of FSI in the PFC could account for the mesocortical-induced prefrontal output inhibition (Tseng *et al*, 2006). We tested this hypothesis and found a non-linear relationship between pyramidal cell firing and FSI. In fact, the mean firing rate of pyramidal neurons begins to increase exponentially when the FSI-dependent GABAergic tone decreases >20%. Interestingly, a reinstatement of the FSI function by augmenting basal dopamine levels was sufficient to reduce the hyperactive PFC state to baseline levels. Thus, one critical mechanism for shaping the activity of PFC output neurons is the responsiveness of FSI to dopamine.

Parvalbumin-positive FSI is the most abundant class of GABAergic cells in the adult PFC (Gabbott *et al*, 1997). As a result of their non-adapting and fast-spiking firing pattern, FSI is functionally positioned to exert fast-feedforward inhibition onto pyramidal neurons and controls the signal detection ratio of the cortical output (Bartos and Elgueta, 2012; Rao *et al*, 2000). Our simulations predict that a proper level of FSI function is required for enabling input-specific processing of afferent information among PFC pyramidal neurons. For example, when the basal dopamine tone is low, the input selectivity begins to deteriorate due to insufficient levels of FSI activity to sustain network stability. Interestingly, too much dopamine tone also reduces PFC selectivity because of excessive inhibition of pyramidal neurons by FSI. Thus, a disruption of FSI function is expected to reduce the PFC capacity for discriminating contextually and emotionally salient signals, in particular those originating from the ventral hippocampus (Abela *et al*, 2012; Chudasama *et al*, 2012; Floresco *et al*, 1997; Seamans *et al*, 1995; Wang and Cai, 2006) and the basolateral amygdala (Davis and Whalen, 2001; Garcia *et al*, 1999; Gilmartin and Helmstetter, 2010; Milad and Quirk, 2012; Morgan and LeDoux, 1995), which are key for the development of mature cognitive abilities associated with adult behavior (Best and Miller, 2010; Casey *et al*, 2000, 2008). In this regard, the well-established role of dopamine on PFC-dependent cognitive functions (see review Floresco, 2013) could be attributable to the fine homeostatic interplay between FSI and dopamine transmission found in our simulations.

Neurocomputational models of PFC function have been successfully used to study neuronal dynamics of dopamine

modulation and working memory (Brunel and Wang, 2001; Durstewitz *et al*, 2000; Tanaka, 2001). Of particular interest is the work by Durstewitz *et al* (2000) wherein the GABAergic component was modeled as a dependent variable of the dopamine's effect, and noticed that concurrent augmentation of the GABA-A conductance in pyramidal neurons is required for proper functioning of the network, in particular to dopamine-driven actions. However, the role of GABA interneurons has never been taken into account as an independent variable in these PFC simulations (see Wang *et al*, 2004) despite the fact that acute blockade of prefrontal GABAergic transmission in animal models has been repeatedly shown to impair cognitive functions within the working memory domain (Enomoto *et al*, 2011; Paine *et al*, 2011; Sawaguchi *et al*, 1988, 1989). Thus, a more pressing question is how dopamine regulation of GABAergic interneurons interplays with the recurrent activity of pyramidal neurons to enable working memory in the PFC, and whether these emerging compensatory mechanisms could be implemented to restore the normal prefrontal output function in pathophysiological conditions of aberrant GABAergic function and/or dopaminergic transmission. By incorporating physiological features of dopamine's action onto FSI (see Discussion above), we have uncovered a range of nonlinear interactions between dopamine and FSI for sustaining an optimal working memory performance. For instance, working memory deficits resulting from downregulation of FSI inhibition can be restored by supra-linearly increasing basal dopamine levels. Results from the simulations also revealed a series of inverted U-shape relationships between working memory and prefrontal dopamine. A similar inverted U-shape function between PFC dopamine and cognition has been often described in animal studies (see review Floresco, 2013), yet the precise neuronal substrate underlying such a relationship remains largely unknown. On the basis of our model, we predict that only an optimal combination of dopamine transmission and FSI function in the PFC will enable appropriate network stability to sustain working memory. In this regard, increasing dopamine tone in the PFC is expected to improve working memory if a functional deficit in local GABAergic transmission is responsible for the sub-optimal prefrontal performance.

In addition to working memory impairments, deficits in prefrontal GABAergic interneurons have been often associated with reduced cognitive flexibility and perseverative behaviors as seen in animal models (Brady, 2009; Gruber *et al*, 2010) as well as in psychiatric disorders including schizophrenia (Lewis and Gonzalez-Burgos, 2006; Uhlhaas and Singer, 2006). Although several mechanisms have been proposed, a common theme thought to account for the lack of behavioral flexibility resulting from prefrontal disinhibition is the inability of the PFC network to reset (Floresco, 2013; Gruber *et al*, 2010). Here, we asked whether features of dopamine–FSI interaction found in our PFC model could have a permissive role to reset prefrontal activity. Results from the simulations indicate that once PFC working memory is formed, a phasic activation of FSI by dopamine (ie, 500 ms) can effectively bring the steady state of working memory-dependent persistent activity down to baseline only if the dopamine transient occurs after the offset of the conditioned stimuli (see Figure 6) and last >350 ms in duration (Supplementary Figure 2). Interestingly, our model also predicts that the level of pyramidal cell inhibition needed to achieve reset requires that activation of FSI surpasses 40 Hz. Thus, a failure to engage sufficient FSI activation is expected to reduce the PFC network cognitive capacity to switch from one state to another. Future studies are warranted to validate these neurocomputational observations in animal models.

In summary, we have presented a neurocomputational model of the PFC that takes into account the often-overlooked role of dopamine modulation of prefrontal GABAergic transmission. This model provides new insights on how the dopaminergic system interacts with both pyramidal neurons and GABAergic interneurons to achieve the complex balance necessary to sustain network stability and input selectivity for the formation and reset of working memory in the PFC.

FUNDING AND DISCLOSURE

The authors declare no conflict of interest.

ACKNOWLEDGEMENTS

This study was supported by Rosalind Franklin University (KYT), the National Institutes of Health Grant R01-MH086507 (KYT), and UBACYT 20020100100902 (SEL). We thank Drs Anthony West and Adriana Caballero for helpful comments.

REFERENCES

Abela AR, Dougherty SD, Fagen ED, Hill CJ, Chudasama Y (2012). Inhibitory control deficits in rats with ventral hippocampal lesions. *Cereb Cortex* **23**: 1396–1409.

Baldwin AE, Sadeghian K, Kelley AE (2002). Appetitive instrumental learning requires coincident activation of NMDA and dopamine D1 receptors within the medial prefrontal cortex. *J Neurosci* **22**: 1063–1071.

Bartos M, Elgueta C (2012). Functional characteristics of parvalbumin- and cholecystokinin-expressing basket cells. *J Physiol* **590**(Pt 4): 669–681.

Best JR, Miller PH (2010). A developmental perspective on executive function. *Child Dev* **81**: 1641–1660.

Brady AM (2009). Neonatal ventral hippocampal lesions disrupt set-shifting ability in adult rats. *Behav Brain Res* **205**: 294–298.

Brunel N, Wang XJ (2001). Effects of neuromodulation in a cortical network model of object working memory dominated by recurrent inhibition. *J Comput Neurosci* **11**: 63–85.

Casey BJ, Giedd JN, Thomas KM (2000). Structural and functional brain development and its relation to cognitive development. *Biol Psychol* **54**: 241–257.

Casey BJ, Jones RM, Hare TA (2008). The adolescent brain. *Ann NY Acad Sci* **1124**: 111–126.

Chudasama Y, Doobay VM, Liu Y (2012). Hippocampal-prefrontal cortical circuit mediates inhibitory response control in the rat. *J Neurosci* **32**: 10915–10924.

Davis M, Whalen PJ (2001). The amygdala: vigilance and emotion. *Mol Psychiatry* **6**: 13–34.

Durstewitz D, Seamans JK, Sejnowski TJ (2000). Dopamine-mediated stabilization of delay-period activity in a network model of prefrontal cortex. *J Neurophysiol* **83**: 1733–1750.

Enomoto T, Tse MT, Floresco SB (2011). Reducing prefrontal gamma-aminobutyric acid activity induces cognitive, behavioral,

and dopaminergic abnormalities that resemble schizophrenia. *Biol Psychiatry* **69**: 432–441.

Ferron A, Thierry AM, Le Douarin C, Glowinski J (1984). Inhibitory influence of the mesocortical dopaminergic system on spontaneous activity or excitatory response induced from the thalamic mediodorsal nucleus in the rat medial prefrontal cortex. *Brain Res* **302**: 257–265.

Flores-Barrera E, Thomases DR, Heng LJ, Cass DK, Caballero A, Tseng KY (2013). Late adolescent expression of GluN2B transmission in the prefrontal cortex is input-specific and requires postsynaptic PKA and D1 dopamine receptor signaling. *Biol Psychiatry* **75**: 508–516.

Floresco SB (2013). Prefrontal dopamine and behavioral flexibility: shifting from an "inverted-U" toward a family of functions. *Front Neurosci* **7**: 62.

Floresco SB, Phillips AG (2001). Delay-dependent modulation of memory retrieval by infusion of a dopamine D1 agonist into the rat medial prefrontal cortex. *Behav Neurosci* **115**: 934–939.

Floresco SB, Seamans JK, Phillips AG (1997). Selective roles for hippocampal, prefrontal cortical, and ventral striatal circuits in radial-arm maze tasks with or without a delay. *J Neurosci* **17**: 1880–1890.

Funahashi S, Bruce CJ, Goldman-Rakic PS (1989). Mnemonic coding of visual space in the monkey's dorsolateral prefrontal cortex. *J Neurophysiol* **61**: 331–349.

Gabbott PL, Dickie BG, Vaid RR, Headlam AJ, Bacon SJ (1997). Local-circuit neurones in the medial prefrontal cortex (areas 25, 32 and 24b) in the rat: morphology and quantitative distribution. *J Comp Neurol* **377**: 465–499.

Garcia R, Vouimba RM, Baudry M, Thompson RF (1999). The amygdala modulates prefrontal cortex activity relative to conditioned fear. *Nature* **402**: 294–296.

Gilmartin MR, Helmstetter FJ (2010). Trace and contextual fear conditioning require neural activity and NMDA receptor-dependent transmission in the medial prefrontal cortex. *Neurobiol Learn Mem* **97**: 452–464.

Goldman-Rakic PS (1995). Cellular basis of working memory. *Neuron* **14**: 477–485.

Gorelova N, Seamans JK, Yang CR (2002). Mechanisms of dopamine activation of fast-spiking interneurons that exert inhibition in rat prefrontal cortex. *J Neurophysiol* **88**: 3150–3166.

Gruber AJ, Calhoon GG, Shusterman I, Schoenbaum G, Roesch MR, O'Donnell P (2010). More is less: a disinhibited prefrontal cortex impairs cognitive flexibility. *J Neurosci* **30**: 17102–17110.

Gulledge AT, Jaffe DB (1998). Dopamine decreases the excitability of layer V pyramidal cells in the rat prefrontal cortex. *J Neurosci* **18**: 9139–9151.

Gurden H, Tassin JP, Jay TM (1999). Integrity of the mesocortical dopaminergic system is necessary for complete expression of in vivo hippocampal-prefrontal cortex long-term potentiation. *Neuroscience* **94**: 1019–1027.

Jay TM (2003). Dopamine: a potential substrate for synaptic plasticity and memory mechanisms. *Prog Neurobiol* **69**: 375–390.

Jay TM, Glowinski J, Thierry AM (1995). Inhibition of hippocampoprefrontal cortex excitatory responses by the mesocortical DA system. *Neuroreport* **6**: 1845–1848.

Le Moine C, Gaspar P (1998). Subpopulations of cortical GABAergic interneurons differ by their expression of D1 and D2 dopamine receptor subtypes. *Brain Res Mol Brain Res* **58**: 231–236.

Lewis BL, O'Donnell P (2000). Ventral tegmental area afferents to the prefrontal cortex maintain membrane potential 'up' states in pyramidal neurons via D(1) dopamine receptors. *Cereb Cortex* **10**: 1168–1175.

Lewis DA, Gonzalez-Burgos G (2006). Pathophysiologically based treatment interventions in schizophrenia. *Nat Med* **12**: 1016–1022.

Lindvall O, Bjorklund A, Moore RY, Stenevi U (1974). Mesencephalic dopamine neurons projecting to neocortex. *Brain Res* **81**: 325–331.

Milad MR, Quirk GJ (2012). Fear extinction as a model for translational neuroscience: ten years of progress. *Annu Rev Psychol* **63**: 129–151.

Morgan MA, LeDoux JE (1995). Differential contribution of dorsal and ventral medial prefrontal cortex to the acquisition and extinction of conditioned fear in rats. *Behav Neurosci* **109**: 681–688.

Mrzljak L, Bergson C, Pappy M, Huff R, Levenson R, Goldman-Rakic PS (1996). Localization of dopamine D4 receptors in GABAergic neurons of the primate brain. *Nature* **381**: 245–248.

Muly EC 3rd, Szigeti K, Goldman-Rakic PS (1998). D1 receptor in interneurons of macaque prefrontal cortex: distribution and subcellular localization. *J Neurosci* **18**: 10553–10565.

O'Donnell P (2011). Adolescent onset of cortical disinhibition in schizophrenia: insights from animal models. *Schizophr Bull* **37**: 484–492.

Paine TA, Slipp LE, Carlezon WA Jr (2011). Schizophrenia-like attentional deficits following blockade of prefrontal cortex GABAA receptors. *Neuropsychopharmacology* **36**: 1703–1713.

Pirot S, Godbout R, Mantz J, Tassin JP, Glowinski J, Thierry AM (1992). Inhibitory effects of ventral tegmental area stimulation on the activity of prefrontal cortical neurons: evidence for the involvement of both dopaminergic and GABAergic components. *Neuroscience* **49**: 857–865.

Rao SG, Williams GV, Goldman-Rakic PS (2000). Destruction and creation of spatial tuning by disinhibition: GABA(A) blockade of prefrontal cortical neurons engaged by working memory. *J Neurosci* **20**: 485–494.

Sawaguchi T, Matsumura M, Kubota K (1988). Delayed response deficit in monkeys by locally disturbed prefrontal neuronal activity by bicuculline. *Behav Brain Res* **31**: 193–198.

Sawaguchi T, Matsumura M, Kubota K (1989). Delayed response deficits produced by local injection of bicuculline into the dorsolateral prefrontal cortex in Japanese macaque monkeys. *Exp Brain Res* **75**: 457–469.

Seamans JK, Floresco SB, Phillips AG (1995). Functional differences between the prelimbic and anterior cingulate regions of the rat prefrontal cortex. *Behav Neurosci* **109**: 1063–1073.

Sesack SR, Hawrylak VA, Matus C, Guido MA, Levey AI (1998). Dopamine axon varicosities in the prelimbic division of the rat prefrontal cortex exhibit sparse immunoreactivity for the dopamine transporter. *J Neurosci* **18**: 2697–2708.

Tanaka S (2001). Computational approaches to the architecture and operations of the prefrontal cortical circuit for working memory. *Prog Neuropsychopharmacol Biol Psychiatry* **25**: 259–281.

Thierry AM, Tassin JP, Blanc G, Glowinski J (1978). Studies on mesocortical dopamine systems. *Adv Biochem Psychopharmacol* **19**: 205–216.

Tseng KY, Chambers RA, Lipska BK (2009). The neonatal ventral hippocampal lesion as a heuristic neurodevelopmental model of schizophrenia. *Behav Brain Res* **204**: 295–305.

Tseng KY, Lewis BL, Hashimoto T, Sesack SR, Kloc M, Lewis DA *et al* (2008). A neonatal ventral hippocampal lesion causes functional deficits in adult prefrontal cortical interneurons. *J Neurosci* **28**: 12691–12699.

Tseng KY, Mallet N, Toreson KL, Le Moine C, Gonon F, O'Donnell P (2006). Excitatory response of prefrontal cortical fast-spiking interneurons to ventral tegmental area stimulation in vivo. *Synapse* **59**: 412–417.

Tseng KY, O'Donnell P (2004). Dopamine-glutamate interactions controlling prefrontal cortical pyramidal cell excitability involve multiple signaling mechanisms. *J Neurosci* **24**: 5131–5139.

Tseng KY, O'Donnell P (2005). Post-pubertal emergence of prefrontal cortical up states induced by D1-NMDA co-activation. *Cereb Cortex* **15**: 49–57.

Tseng KY, O'Donnell P (2007a). D2 dopamine receptors recruit a GABA component for their attenuation of excitatory synaptic transmission in the adult rat prefrontal cortex. *Synapse* **61**: 843–850.

Tseng KY, O'Donnell P (2007b). Dopamine modulation of prefrontal cortical interneurons changes during adolescence. *Cereb Cortex* **17**: 1235–1240.

Uhlhaas PJ, Singer W (2006). Neural synchrony in brain disorders: relevance for cognitive dysfunctions and pathophysiology. *Neuron* **52**: 155–168.

Vincent SL, Khan Y, Benes FM (1995). Cellular colocalization of dopamine D1 and D2 receptors in rat medial prefrontal cortex. *Synapse* **19**: 112–120.

Wang GW, Cai JX (2006). Disconnection of the hippocampal-prefrontal cortical circuits impairs spatial working memory performance in rats. *Behav Brain Res* **175**: 329–336.

Wang XJ, Tegner J, Constantinidis C, Goldman-Rakic PS (2004). Division of labor among distinct subtypes of inhibitory neurons in a cortical microcircuit of working memory. *Proc Natl Acad Sci USA* **101**: 1368–1373.

Supplementary Information accompanies the paper on the Neuropsychopharmacology website (http://www.nature.com/npp)